hep-ph/yymmnnn

Neutrino Oscillation Phenomenology

Stephen J. Parke*

Theoretical Physics Department,
Fermi National Accelerator Laboratory,
P. O. Box 500, Batavia, IL 60510, USA

(Dated: August 13, 2007)

Abstract

A summary of neutrino oscillation phenomenology is given within the context of the neutrino Standard Model (3 active flavors only) for both the disappearance and appearance modes. Extensions of the model to include one of more sterile neutrinos is included.

PACS numbers: 14.60.Pq,76.80.+y

*Electronic address: `parke@fnal.gov`

I. INTRODUCTION

In the Standard Model the neutrinos, $(\nu_e,\ \nu_\mu,\ \nu_\tau)$, are massless and interact diagonally in flavor, as follows

$$\begin{array}{ccc} W^+ \to e^+ + \nu_e & W^- \to e^- + \bar{\nu}_e & Z \to \nu_e + \bar{\nu}_e \\ W^+ \to \mu^+ + \nu_\mu & W^- \to \mu^- + \bar{\nu}_\mu & Z \to \nu_\mu + \bar{\nu}_\mu \\ W^+ \to \tau^+ + \nu_\tau & W^- \to \tau^- + \bar{\nu}_\tau & Z \to \nu_\tau + \bar{\nu}_\tau . \end{array} \tag{1}$$

Since they travel at the speed of light, their character cannot change from production to detection. Therefore, in flavor terms, massless neutrinos are relatively uninteresting compared to quarks.

Many experiments have seen neutrino flavor transitions, therefore neutrinos must have mass and, like the quarks, there is a mixing matrix relating the flavor states with the mass eigenstates:

$$|\nu_\alpha\rangle = U_{\alpha j}|\nu_j\rangle, \tag{2}$$

where $\nu_\alpha = (\nu_e,\ \nu_\mu,\ \nu_\tau, \ldots)$, represent the flavor states and $\nu_j = (\nu_1,\ \nu_2,\ \nu_3, \ldots)$ represent the mass eigenstates with mass m_j. The mixing matrix $U_{\alpha j}$ is usually called the MNS mixing matrix, see [1].

Except for the LSND anomaly, all neutrino data can be explained by the following neutrino Standard Model:

- 3 light (m_i <1 eV) Neutrinos: (probably Majorana)
  $\Rightarrow$ only 2 independent δm^2 ($\delta m^2_{ij} = m_i^2 - m_j^2$)
- Three active neutrino flavors (no steriles): $\nu_e,\ \nu_\mu,\ \nu_\tau$
- Unitary Mixing Matrix:
  3 angles $(\theta_{12},\ \theta_{23},\ \theta_{13})$, 1 Dirac phase (δ), 2 Majorana phases (α, β)

where the MNS mixing matrix relating flavor to mass eigenstates, is given by

$$U_{\alpha i} = \begin{pmatrix} 1 & & \\ & c_{23} & s_{23} \\ & -s_{23} & c_{23} \end{pmatrix} \begin{pmatrix} c_{13} & & s_{13}e^{-i\delta} \\ & 1 & \\ -s_{13}e^{i\delta} & & c_{13} \end{pmatrix} \begin{pmatrix} c_{12} & s_{12} & \\ -s_{12} & c_{12} & \\ & & 1 \end{pmatrix} \begin{pmatrix} 1 & & \\ & e^{i\alpha} & \\ & & e^{i\beta} \end{pmatrix} \tag{3}$$

$$= \begin{pmatrix} c_{13}c_{12} & c_{13}s_{12} & s_{13}e^{-i\delta} \\ -c_{23}s_{12} - s_{13}c_{12}s_{23}e^{+i\delta} & c_{23}c_{12} - s_{13}s_{12}s_{23}e^{+i\delta} & c_{13}s_{23} \\ s_{23}s_{12} - s_{13}c_{12}c_{23}e^{+i\delta} & -s_{23}c_{12} - s_{13}s_{12}c_{23}e^{+i\delta} & c_{13}c_{23} \end{pmatrix} \begin{pmatrix} 1 & & \\ & e^{i\alpha} & \\ & & e^{i\beta} \end{pmatrix}$$

where $s_{ij} = \sin\theta_{ij}$ and $c_{ij} = \cos\theta_{ij}$. The (23) sector is identified with the atmospheric δm^2_{atm} and the (12) sector is identified with the solar $\delta m^2_\odot$. The (13) sector is responsible for the ν_e flavor transitions at the atmospheric scale so far unobserved. The Dirac phase, δ, allows for the possibility of CP violation in the appearance modes. The current best fit values or

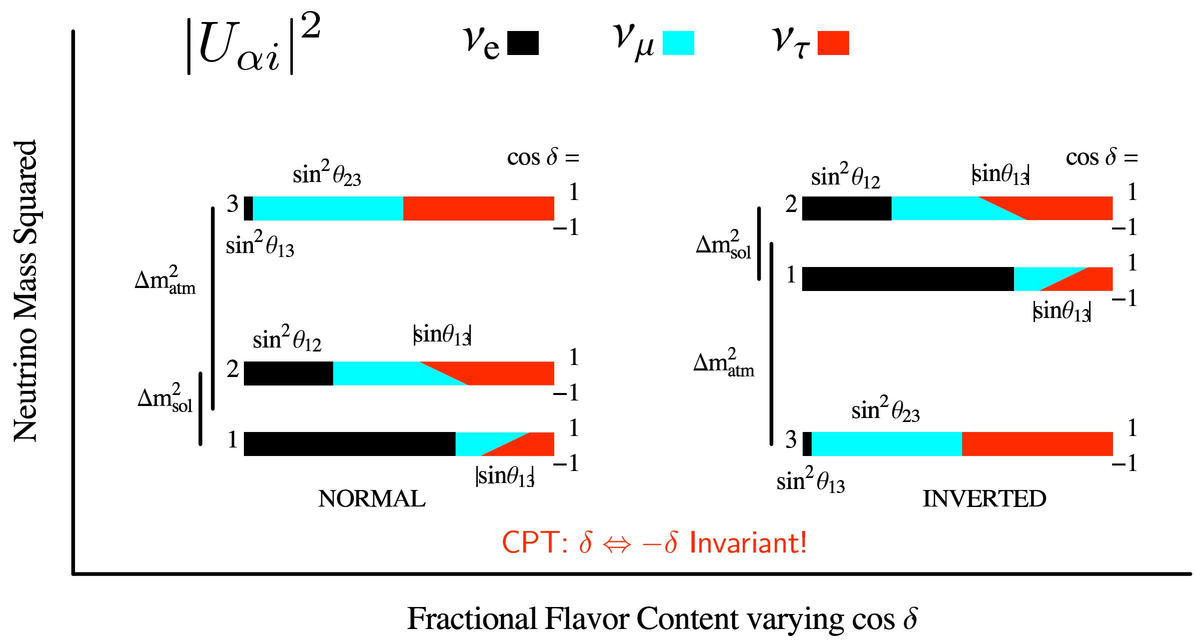

FIG. 1: Flavor content of the three neutrino mass eigenstates showing the dependence on the cosine of the CP violating phase, δ. If CPT is conserved, the flavor content must be the same for neutrinos and anti-neutrinos. This figure was adapted from Ref. [4].

limits, see [3], on these parameters are[1]

$$\begin{aligned} \sin^2\theta_{12} &= 0.31 \pm 0.03 \\ \sin^2\theta_{23} &= 0.50 \pm 0.15 \\ \sin^2\theta_{13} &< 0.04 \\ 0 \leq \delta &< 2\pi \end{aligned}$$

and the mass splittings are approximately

$$|\delta m^2_{32}| = 2.7 \pm 0.4 \times 10^{-3}\text{eV}^2 \quad \text{and} \quad \delta m^2_{21} = +8.0 \pm 0.4 \times 10^{-5}\text{eV}^2.$$

The mass of the lightest neutrino is unknown but the heaviest one must be lighter than about 1 eV. These mixing angles and mass splittings are summarized in Fig. 1 which also shows the dependence of the flavor fractions on the CP violating Dirac phase, δ. The Majorana phases are unobservable in oscillations since oscillations depend on $U^*_{\alpha i}U_{\beta i}$ but they have observable, CP conserving effects, in neutrinoless double beta decay. If the neutrinos are Dirac, then neutrinoless double beta decay will be unobserved and the Majorana phases in the MNS matrix are unobservable and can be set to zero.

The unresolved questions within this model that can addressed in oscillation experiments are

[1] Some experiments report their results in terms of $\sin^2(2\theta)$, others in terms of $\tan^2\theta$. However, $\sin^2\theta$ is used here, since each of the three $\sin^2\theta$'s approximately corresponds to the fraction of a certain flavor in one of the mass eigenstates as follows: $\sin^2\theta_{13} = |U_{e3}|^2 \ll 1$, $\sin^2\theta_{23} \approx |U_{\mu 3}|^2$ and $\sin^2\theta_{12} \approx |U_{e2}|^2$.

- What is the size of $|U_{e3}|^2$? i.e $\sin^2\theta_{13}$?
- Hierarchy: Is $m_3^2 >$ OR $< m_1^2$? sign δm_{31}^2 ?
- Is CP violation? $\sin\delta \neq 0$.
- Is $|U_{\mu 3}|^2 = |U_{\tau 3}|^2$? i.e. $\sin^2\theta_{23} = \frac{1}{2}$?
  If not, is $|U_{\mu 3}|^2 >$ or $< |U_{\tau 3}|^2$? i.e. $\sin^2\theta_{23} >$ or $< \frac{1}{2}$?

Other important questions include:

- Are Neutrinos Majorana or Dirac ?
- Are there more than three neutrinos? Sterile Neutrinos.
- Do exotic neutrinos interactions exist?
- What is the mass of lightest neutrino?

II. THE ν_e DISAPPEARANCE CHANNEL

For massive neutrinos the disappearance probability for any flavor is given by

$$\begin{aligned} P(\nu_\alpha \to \nu_\alpha) &= P(\bar\nu_\alpha \to \bar\nu_\alpha) \\ &= \left| \sum_j U^*_{\alpha j} e^{-im_j^2 L/2E} U_{\alpha j} \right|^2 . \end{aligned} \tag{4}$$

That is, the square of the sum of the amplitudes for the α flavor neutrino to produce a m_j mass state times a propogator factor times the amplitude for the m_j mass states to produce the α flavor neutrino. Invariance under CPT forces the disappearance probability for neutrinos and anti-neutrinos to be identical, in vacuum.

In the three flavor neutrino Standard Model this can written as

$$P(\nu_e \to \nu_e) = 1 - 4|U_{e3}|^2|U_{e1}|^2 \sin^2\Delta_{31} - 4|U_{e3}|^2|U_{e2}|^2 \sin^2\Delta_{32} - 4|U_{e2}|^2|U_{e1}|^2 \sin^2\Delta_{21} \tag{5}$$

where the kinematic phase is given by

$$\Delta_{jk} \equiv \frac{\delta m_{jk}^2 L}{4\hbar c E} = 1.2669\cdots \left(\frac{\delta m_{jk}^2}{eV^2}\right)\left(\frac{L}{km}\right)\left(\frac{GeV}{E}\right) \tag{6}$$

and the unitarity properties of the MNS matrix have been used.

A. Reactor Experiments at the Solar L/E:

For experiments at the solar L/E (around 15km/MeV) without the resolution to resolve the atmospheric oscillations on top of the dominant solar oscillation, such as KamLAND Ref. [5], Eq. 5 can be written as

$$P(\bar\nu_e \to \bar\nu_e) = c_{13}^4(1 - \sin^2 2\theta_{12} \sin^2\Delta_{21}) + s_{13}^4. \tag{7}$$

Since s_{13}^4 is known to be very small, $< 10^{-3}$, the only effect of non-zero θ_{13} is a multiplicative reduction of the disappearance probability. To measure this overall reduction requires precise knowledge of the neutrino flux from the reactor(s). However, the solar parameters and in particular δm_{21}^2 can be measured with high precision in such an experiment.

B. Reactor Experiments at the Atmospheric L/E:

For experiments at the atmospheric L/E (around 0.5 km/MeV), such as Chooz[6], Palo Verde[7], Double-CHOOZ[8] and Daya Bay[9], the disappearance probability, Eq. 5, can be written as

$$P(\bar{\nu}_e \rightarrow \bar{\nu}_e) \;=\; 1 - \sin^2 2\theta_{13} \sin^2 \Delta_{ee} + \mathcal{O}(\Delta_{21}^2) \tag{8}$$

where $\Delta_{ee} = \delta m^2_{ee} L/4E$. δm^2_{ee} is the effective atmospheric δm^2 for the ν_e disappearance channel, see Ref. [10], given by

$$\delta m^2_{ee} \equiv c^2_{12}|\delta m^2_{31}| + s^2_{12}|\delta m^2_{32}|. \tag{9}$$

That is, the electron flavor weighted average of δm^2_{31} and δm^2_{32}. The experiments Double Chooz and Di Baya are designed to measure or put a limit on the size of $\sin^2\theta_{13}$ significantly below the current limit of

$$\sin^2\theta_{13} < 0.04 \tag{10}$$

at the best fit value for the atmospheric δm^2.

C. Solar Neutrinos

Solar neutrinos are somewhat more complicated because of the matter effects that the neutrinos experience from the production region until they exit the sun, at least for the ^{8}Boron neutrinos. The pp and ^{7}Be neutrinos are little effected by the matter and undergo quasi-vacuum oscillations whereas the ^{8}Boron neutrinos produced and exit the sun mainly as a ν_2 mass eigenstate because of matter effects and therefore do not undergo oscillations. This difference is primarily due to the difference in the energy of the neutrinos: pp (^{7}Be) have a mean energy of 0.2 MeV (0.9 MeV) whereas ^{8}B have a mean energy of 10 MeV and the matter effect is proportional to energy of the neutrino.

The kinematic phase for solar neutrinos is

$$\Delta_\odot = \frac{\delta m^2_\odot L}{4E} = 10^{7\pm1}. \tag{11}$$

Therefore, the solar neutrinos are "effectively incoherent" when they reach the earth. Hence the ν_e survival or disappearance probability is given by

$$\begin{aligned} \langle P(\nu_e \rightarrow \nu_e)\rangle \;&=\; f_1 \cos^2\theta_\odot + f_2 \sin^2\theta_\odot \\ \text{where} \quad f_1 + f_2 \;&=\; 1 \quad \text{and} \quad \cos^2\theta_\odot + \sin^2\theta_\odot = 1, \end{aligned} \tag{12}$$

where f_1 and f_2 are the fraction of neutrinos that are ν_1 and ν_2 respectively. Now the pp and ^{7}Be solar neutrinos behave essentially as in vacuum[2] and therefore $f_1 \approx \cos^2\theta_\odot = 0.69$ and $f_2 \approx \sin^2\theta_\odot = 0.31$ whereas the mass eigenstate fraction for the ^{8}B are substantially different, $f_2 \approx 0.9$ due to Mikheyev-Smirnov-Wolfenstein, Ref. [11], matter effects, see Fig. 2.

[2] In vacuum, a ν_e has a ν_1 fraction equal to $\cos^2\theta_\odot$ and a ν_2 fraction equal to $\sin^2\theta_\odot$. Whereas, the probability of finding a ν_e in a ν_1 is $\cos^2\theta_\odot$. For a ν_2, the ν_e fraction is $\sin^2\theta_\odot$.

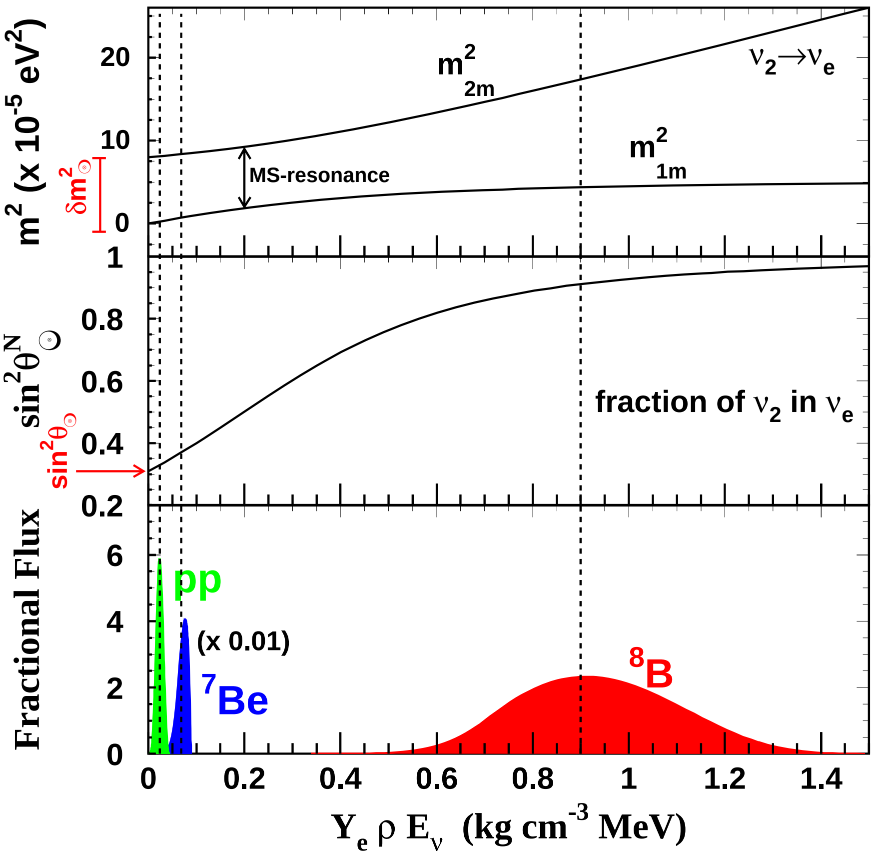

FIG. 2: The Mass spectrum (top panel), the fraction of ν_2's produced, $\sin^2\theta^N_\odot$, (middle panel) and the fractional flux (bottom panel) versus the product of the electron fraction, Y_e, the matter density, ρ, and the neutrino energy, E_ν, for the best fit values $\delta m^2_\odot = 8.0 \times 10^{-5}\mathrm{eV}^2$ and $\sin^2\theta_\odot = 0.310$. The vertical dashed lines give the value of $Y_e\rho E_\nu$ which reproduces the average ν_2 fractions, 91, 37 and 33% for ^{8}B, ^{7}Be and pp respectively. This value of $Y_e\rho E_\nu = 0.89$ kg cm^{-3} MeV, for the ^{8}B neutrinos, gives a production mixing angle equal to 73° and a production $\delta m^2_N = 13 \times 10^{-5}$ eV^2. The matter potential, A, is related to density factor, $Y_e\rho E_\nu$, by $A \equiv 2\sqrt{2}G_F(Y_e\rho/M_n)E_\nu = 15.3 \times 10^{-5}\mathrm{eV}^2 \left(Y_e\rho\ E_\nu/\mathrm{kg.cm}^{-3}.\mathrm{MeV}\right)$. For details see [14].

In a two neutrino analysis, the *day-time* CC/NC of SNO, which is equivalent to the day-time average ν_e survival probability, $\langle P(\nu_e \to \nu_e)\rangle$, is given by

$$\left.\frac{\mathrm{CC}}{\mathrm{NC}}\right|_{\mathrm{day}} = \langle P(\nu_e \to \nu_e)\rangle = \sin^2\theta_\odot + f_1 \cos 2\theta_\odot, \tag{13}$$

where f_1 and $f_2 = 1 - f_1$ are understood to be the ν_1 and ν_2 fractions, respectively, averaged over the ^{8}B neutrino energy spectrum weighted with the charged current cross section. Therefore, the ν_1 fraction (or how much f_2 differs from 100%) is given by

$$f_1 = \frac{\left(\left.\frac{\mathrm{CC}}{\mathrm{NC}}\right|_{\mathrm{day}} - \sin^2\theta_\odot\right)}{\cos 2\theta_\odot} = \frac{(0.347 - 0.311)}{0.378} \approx 10\ \%, \tag{14}$$

where the central values of the recent SNO analysis, [12], have been used.

How does this come about? As the neutrino propogates in matter, the electron neutrino plays a special role due to the forward scattering of the electron neutrino on the electrons in the matter coming from W-bosons exchange, i.e. the charge current interaction[3]. This additional contribution to the Hamiltonian from ν_e+e scattering is $-\sqrt{2}G_F N_e$ which appears only for the electron neutrino. For $\bar{\nu}_e + e$ scattering the sign is flipped. G_F is the Fermi constant and N_e is the number density of electrons in matter. This implies that the matter mass eigenstates are different than the vacuum mass eigenstates and that the Δm^2 and mixing angle, θ, in matter are relates to their vacuum values as follows:

$$\begin{aligned} \Delta m^2_N \cos 2\theta_N &= \Delta m^2_0 \cos 2\theta_0 - 2\sqrt{2}G_F N_e E_\nu \\ \Delta m^2_N \sin 2\theta_N &= \Delta m^2_0 \sin 2\theta_0. \end{aligned} \tag{15}$$

The subscript on Δm^2 and θ denotes the value of the number density of electrons. For large values of the number density of electrons, the mixing angle in matter, θ_N, approaches $\pi/2$. Thus, the higher neutrino mass state becomes nearly completely ν_e. The minimum value of Δm^2_N occurs when $\Delta m^2_0 \cos 2\theta_0 = 2\sqrt{2}G_F N_e E_\nu$ and $\theta_N = \pi/4$. This point is known as the Mikheyev-Smirnov resonance.

For solar neutrinos the matter effects on Δm^2 and θ are shown in Fig. 2. As the number density[4] times energy of the neutrinos gets larger the mixing angle approaches $\pi/2$ and the Δm^2 approaches $2\sqrt{2}G_F N_e E_\nu$. Therefore, a solar ν_e born in an environment with high $2\sqrt{2}G_F N_e E_\nu$ is approximately born as a ν_2 matter mass eigenstate!

Using the analytical analysis of the MSW effect given in Ref. [13], the mass eigenstate fractions are given by

$$f_2 = 1 - f_1 \;=\; \langle \sin^2\theta^N_\odot + P_x \cos 2\theta^N_\odot \rangle_{^8\mathrm{B}}, \tag{16}$$

where $\theta^N_\odot$ is the mixing angle defined at the ν_e production point and P_x is the probability of the neutrino to jump from one mass eigenstate to the other during the Mikheyev-Smirnov (MS) resonance crossing. In the large mixing angle region P_x is zero to high precision. The average $\langle \cdots \rangle_{^8\mathrm{B}}$ is over the electron density of the ^{8}B ν_e production region in the center of the Sun predicted by the Standard Solar Model and the energy spectrum of ^{8}B neutrinos weighted with SNO's charged current cross section. Thus, the ^{8}B energy weighted average fraction of ν_2's observed by SNO, see [14], is

$$\begin{aligned} f_2 &= \langle \sin^2\theta^N_\odot \rangle_{^8\mathrm{B}} = \frac{1}{2} + \frac{1}{2}\left\langle \frac{(A - \delta m^2_\odot \cos 2\theta_\odot)}{\sqrt{(\delta m^2_\odot \cos 2\theta_\odot - A)^2 + (\delta m^2_\odot \sin 2\theta_\odot)^2}} \right\rangle_{^8\mathrm{B}} \\ &= 91 \pm 2\% \quad \text{at the 95\% CL}, \end{aligned} \tag{17}$$

where $A = 2\sqrt{2}G_F(Y_e\rho/M_n)E_\nu$. Hence, the ^{8}B solar neutrinos are the purest mass eigenstate neutrino beam known so far and SK's, Ref. [15], famous picture of the sun taken with neutrinos is more than 80% ν_2 !!!

[3] Interactions via the Z-bosons are the same for all flavors and therefore effect all neutrinos equally.

[4] $N_e = \rho Y_e/M_n$ where Y_e is the electron fraction, ρ is the density and M_n is the nucleon mass.

III. THE ν_μ DISAPPEARANCE CHANNEL

In vacuum, the ν_μ disappearance probability is given by

$$P(\nu_\mu \to \nu_\mu) \;=\; 1 - 4|U_{\mu 3}|^2|U_{\mu 1}|^2 \sin^2\Delta_{31} - 4|U_{\mu 3}|^2|U_{\mu 2}|^2 \sin^2\Delta_{32} - 4|U_{\mu 2}|^2|U_{\mu 1}|^2 \sin^2\Delta_{21}. \quad (18)$$

A. Around the First Oscillation Minima

For experiments at the atmospheric L/E (around 500 km/GeV), such as K2K [16], Minos [16], T2K [18] and NOνA [19] in $\nu_\mu \to \nu_\mu$ mode , Eq. 18, can be written as

$$P(\nu_\mu \to \nu_\mu) \;=\; 1 - 4|U_{\mu 3}|^2(1 - |U_{\mu 3}|^2)\sin^2\Delta_{\mu\mu} + \mathcal{O}(\Delta_{21}^2) \quad (19)$$

where $|U_{\mu 3}|^2 = c_{13}^2 s_{23}^2$ and $\Delta_{\mu\mu} = \delta m^2_{\mu\mu} L/4E$. $\delta m^2_{\mu\mu}$ is the effective atmospheric δm^2 for the ν_μ disappearance channel[5] given by

$$\delta m^2_{\mu\mu} \equiv \frac{|U_{\mu 1}|^2|\delta m^2_{31}| + |U_{\mu 2}|^2|\delta m^2_{32}|}{(|U_{\mu 1}|^2 + |U_{\mu 2}|^2)}, \quad (20)$$

i.e. the muon flavor weighted average of δm^2_{31} and δm^2_{32}. In the limit that $\theta_{13} \to 0$

$$4|U_{\mu 3}|^2(1 - |U_{\mu 3}|^2) \;=\; \sin^2 2\theta_{23} \quad (21)$$
$$\text{and} \quad \delta m^2_{\mu\mu} \;=\; s_{12}^2|\delta m^2_{31}| + c_{12}^2|\delta m^2_{32}| \quad (22)$$

The difference between $\delta m^2_{\mu\mu}$ and $|\delta m^2_{32}|$ is given by $\pm s_{12}^2 \delta m^2_{21}$ which is approximately a 1% shift whose sign depends on the hierarchy. This form of the oscillation probability is what SK uses in their two flavor analysis of atmospheric neutrinos.

IV. APPEARANCE CHANNELS: $\nu_\mu \to \nu_e$

The most likely genuine three flavor effects to be first observed are long baseline $\nu_\mu \to \nu_e$ or one of its CP and T conjugate processes. That is, in one of following transitions

$$\begin{array}{ccccc} & & \text{CP} & & \\ & \nu_\mu \to \nu_e & \Longleftrightarrow & \bar\nu_\mu \to \bar\nu_e & \\ \text{T} & \Updownarrow & & \Updownarrow & \text{T} \\ & \nu_e \to \nu_\mu & \Longleftrightarrow & \bar\nu_e \to \bar\nu_\mu & \\ & & \text{CP} & & \end{array}$$

[5] The difference between the two effective atmospheric δm^2 is small and depends on the hierarchy. $\delta m^2_{ee} - \delta m^2_{\mu\mu} = \pm \delta m^2_{21}(\cos 2\theta_{12} - \cos\delta \sin\theta_{13} \sin 2\theta_{12} \tan\theta_{23})$ where the + (-) is for the normal (inverted) hierarchies, see [10].

Processes across the diagonal are related by CPT. The first row will be explored in very powerful conventional beams, Superbeams, whereas the second row could be explored in Nu-Factories or Beta Beams.

In vacuum, the probability for $\nu_\mu \to \nu_e$ is derived like so, [20],

$$\begin{aligned} P(\nu_\mu \to \nu_e) &= \mid U^*_{\mu 1} e^{-im_1^2 L/2E} U_{e1} + U^*_{\mu 2} e^{-im_2^2 L/2E} U_{e2} + U^*_{\mu 3} e^{-im_3^2 L/2E} U_{e3} \mid^2 \\ &= |2U^*_{\mu 3} U_{e3} \sin\Delta_{31} e^{-i\Delta_{32}} + 2U^*_{\mu 2} U_{e2} \sin\Delta_{21}|^2 \\ &\approx |\sqrt{P_{atm}} e^{-i(\Delta_{32}+\delta)} + \sqrt{P_{sol}}|^2 \end{aligned} \tag{23}$$

where $\sqrt{P_{atm}} = \sin\theta_{23} \sin 2\theta_{13} \sin\Delta_{31}$ and $\sqrt{P_{sol}} \approx \cos\theta_{23} \sin 2\theta_{12} \sin\Delta_{21}$. For anti-neutrinos δ must be replaced with $-\delta$ and the interference term changes

$$2\sqrt{P_{atm}}\sqrt{P_{sol}} \cos(\Delta_{32}+\delta) \;\Rightarrow\; 2\sqrt{P_{atm}}\sqrt{P_{sol}} \cos(\Delta_{32}-\delta).$$

Expanding $\cos(\Delta_{32} \pm \delta)$, one has a CP conserving part

$$2\sqrt{P_{\rm atm}}\sqrt{P_{\rm sol}} \cos\Delta_{32} \cos\delta \tag{24}$$

and the CP violating part

$$\mp 2\sqrt{P_{\rm atm}}\sqrt{P_{\rm sol}} \sin\Delta_{32} \sin\delta, \tag{25}$$

where - (+) sign is for neutrino (anti-neutrino). This allows for the possibility that CP violation maybe able to be observed in the neutrino sector since it allows for $P(\nu_\mu \to \nu_e) \neq P(\bar{\nu}_\mu \to \bar{\nu}_e)$.

In matter, $\sqrt{P_{atm}}$ and $\sqrt{P_{sol}}$ are modified as follows

$$\begin{aligned} \sqrt{P_{atm}} &\Rightarrow \sin\theta_{23} \sin 2\theta_{13} \frac{\sin(\Delta_{31}-aL)}{(\Delta_{31}-aL)} \Delta_{31} \\ \sqrt{P_{sol}} &\Rightarrow \cos\theta_{23} \sin 2\theta_{12} \frac{\sin(aL)}{(aL)} \Delta_{21} \end{aligned} \tag{26}$$

where $a = \pm G_F N_e/\sqrt{2} \approx (4000\ km)^{-1}$ and the sign is positive for neutrinos and negative for anti-neutrinos. This change follows since in both the (31) and (21) sectors the product $\{\delta m^2 \sin 2\theta\}$ is approximately independent of matter effects. Figure 3 shows the ν_e appearance probability as a function of the distance for neutrinos and anti-neutrinos for both mass orderings at an energy appropriate for T2K, E=0.6 GeV. Whereas, Fig. 4 is the ν_e appearance probability as a function of the neutrino energy at a distance appropriate for NOνA, L=810 km. In Figs 5 and 6 the bi-probability plots are shown for both T2K, [18], and NOνA, [19] . It is possible that these two experiments will determine the mass ordering (normal or inverted hierarchy, see Fig. 1), and observe CP violation in the neutrino sector.

V. BEYOND THE NEUTRINO STANDARD MODEL:

Except for the LSND anomaly [21], all neutrino flavor transitions observed so far can be explain using three massive neutrinos which are orthogonal mixtures of the three neutrinos of given flavor. The LSND anomaly is the observation of $\bar{\nu}_\mu \to \bar{\nu}_e$ at an L/E of order

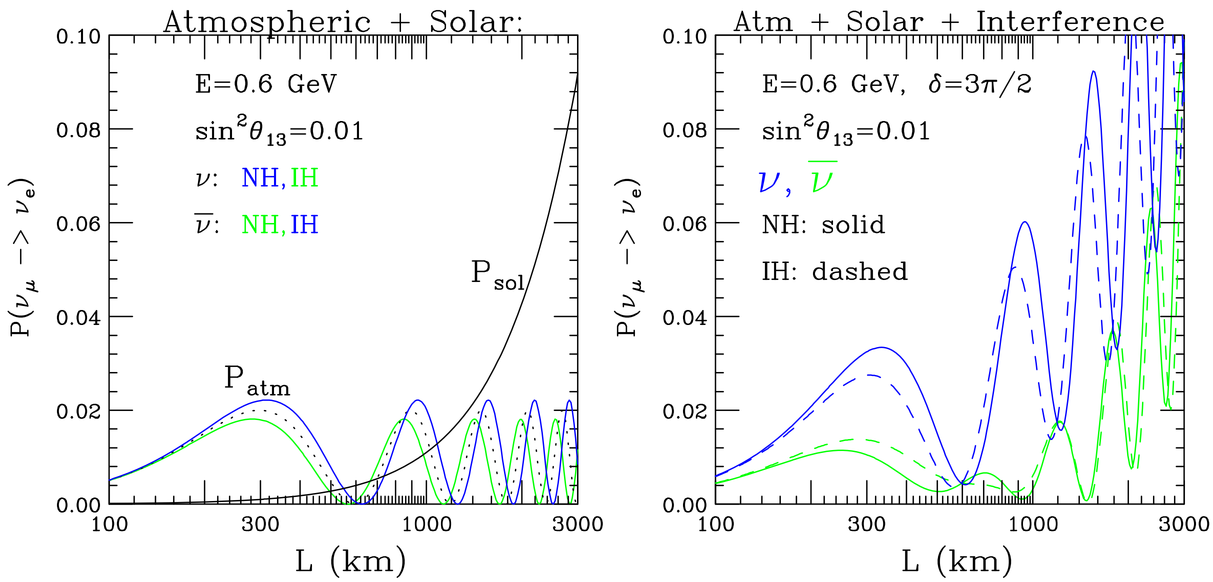

FIG. 3: The left panel show the atmospheric and solar components of the ν_e appearance probability for a neutrino energy of 0.6 GeV for both neutrinos and anti-neutrinos and both mass orderings as a function of the baseline. The dotted P_{atm} curve is the vacuum atmospheric appearance probability. P_{sol} is independent of the hierarchy and the same for neutrinos and anti-neutrinos. The T2K experiment will be performed at approximately this energy at a distance of 295 km and, if constructed, T2KK will be around 1000 km. The right panel shows the full appearance probability including the interference term for $\delta = 3\pi/2$. The appearance probabilities for $\delta = \pi/2$ can be obtained from these by interchanging normal and inverted as well as neutrinos and anti-neutrinos.

500m/GeV with a transition probability of 0.2 %. This suggested the possibility of one or more addition neutrinos which have a squared mass splitting from the active neutrinos of order 1 eV^2. These additional light neutrinos cannot have $SU(2)\times U(1)$ quantum numbers otherwise their effects would have been observed in other processes, e.g. the decay of Z-boson. Hence, they are called sterile neutrinos. One additional sterile neutrino is marginally compatible with all existing data in the 3+1 scenario[6]. The strongest constraints on this model come from ν_e and ν_μ disappearance experiments. The disappearance of ν_e at the LSND L/E depends on the fraction, $|U_{e4}|^2$, of ν_e in the additional 4th-neutrino and similar for ν_μ. The non-obersevation of disappearance of both ν_e and ν_μ implies that both $|U_{e4}|^2$ and $|U_{\mu 4}|^2$ are small. In this 3+1 model, the LSND appearance of $\bar{\nu}_e$ from $\bar{\nu}_\mu$ depends on the product of these two small quantities, $|U_{e4}|^2|U_{\mu 4}|^2$. Thus, moderate limits on the disappearance modes can severely constraint the appearance mode. In a full analysis of both the disappearance and appearance channels only a few small atolls are not excluded at high confidence level in the $\{\delta m^2 \text{ v } \sin^2 2\theta\}_{LSND}$ plane. The 2+2 scenario[7] is strongly disfavored, since both the solar and atmospheric oscillations are primarily due to active neutrino oscillations. In this model one or both of these phenomena would have to have a substantial sterile neutrino component.

What about the possibility of more than one sterile neutrino? With two or more addi-

[6] In the 3+1 model the additional neutrino is split from the other neutrinos by order of 1 eV^2.

[7] In the 2+2 model the solar neutrino pair is split from the atmospheric neutrino pair by order of 1 eV^2.

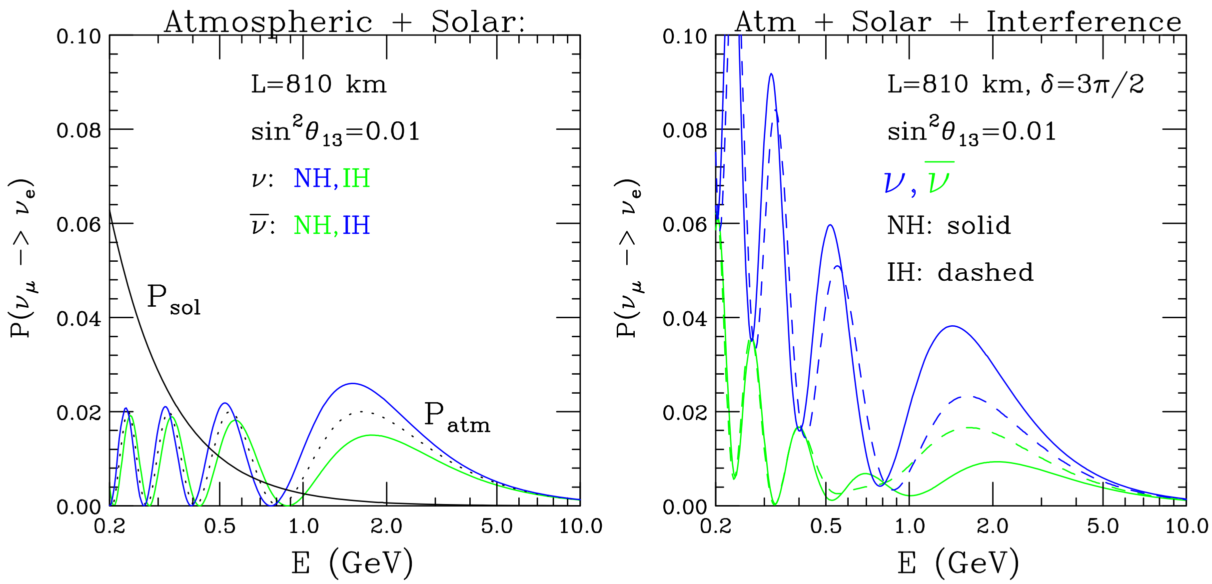

FIG. 4: The left panel show the atmospheric and solar components of the ν_e appearance probability at a distance of 810 km for both neutrinos and anti-neutrinos and both mass orderings as a fuction of the neutrino energy. The dotted P_{atm} curve is the vacuum atmospheric appearance probability. P_{sol} is independent of the hierarchy and the same for neutrinos and anti-neutrinos. The NOνA experiment will be performed at this distance with an energy centered at 2 GeV. If an experiment is mounted at the second oscillation maximum at this distance the energy would be approximately 0.6 GeV. The right panel shows the full appearance probability including the interference term for $\delta = 3\pi/2$. The appearance probabilities for $\delta = \pi/2$ can be obtained from these by interchanging normal and inverted as well as neutrinos for anti-neutrinos.

tional neutrinos the parameters can be chosen so as to be compatible with all existing data, even with the recent non-observation by mini-BOONE [22] of $\nu_\mu \to \nu_e$ at the same L/E and sensitivity as LSND, see [23]. This can occur because of the possibility of CP violation at the LSND L/E in models with two or more additional neutrinos. Let us consider the 3+2 model is some detail. If we label the masses of the two additional neutrinos m_4 and m_5 then following Eq. 23,

$$\begin{aligned} P(\nu_\mu \to \nu_e) &= |2U^*_{\mu 5}U_{e5}\sin\Delta_{51}e^{-i\Delta_{54}} + 2U^*_{\mu 4}U_{e4}\sin\Delta_{41}|^2 \\ &= 4|U_{\mu 5}|^2|U_{e5}|^2\sin^2\Delta_{51} + 4|U_{\mu 4}|^2|U_{e4}|^2\sin^2\Delta_{41} \\ &\quad +8|U_{\mu 5}||U_{e5}||U_{\mu 4}||U_{e4}|\sin\Delta_{51}\sin\Delta_{41}\cos(\Delta_{54}+\delta_{54}) \end{aligned} \tag{27}$$

where $\delta_{54} = \pm\arg(U^*_{\mu 5}U_{e5}U_{\mu 4}U^*_{e4})$. The positive sign is for $\nu_\mu \to \nu_e$ whereas the negative sign is for $\bar{\nu}_\mu \to \bar{\nu}_e$. At the LSND L/E the difference between the masses, m_1, m_2 and m_3 is too small to be relevant, so m_1 has been used as the common mass of these neutrinos, i.e. $\Delta_{51} \approx \Delta_{52} \approx \Delta_{53}$ and $\Delta_{41} \approx \Delta_{42} \approx \Delta_{43}$. The last term of Eq. 27 is the interference term between the two amplitudes which can be constructive for $\bar{\nu}_\mu \to \bar{\nu}_e$ and destructive for $\nu_\mu \to \nu_e$. Therefore allowing for the possibility that

$$P(\bar{\nu}_\mu \to \bar{\nu}_e) \; > \; P(\nu_\mu \to \nu_e). \tag{28}$$

This is a possible explanation of why LSND sees a signal in anti-neutrinos whereas mini-BOONE does not see a signal in neutrinos at approximately the same sensitivity. The ν_e

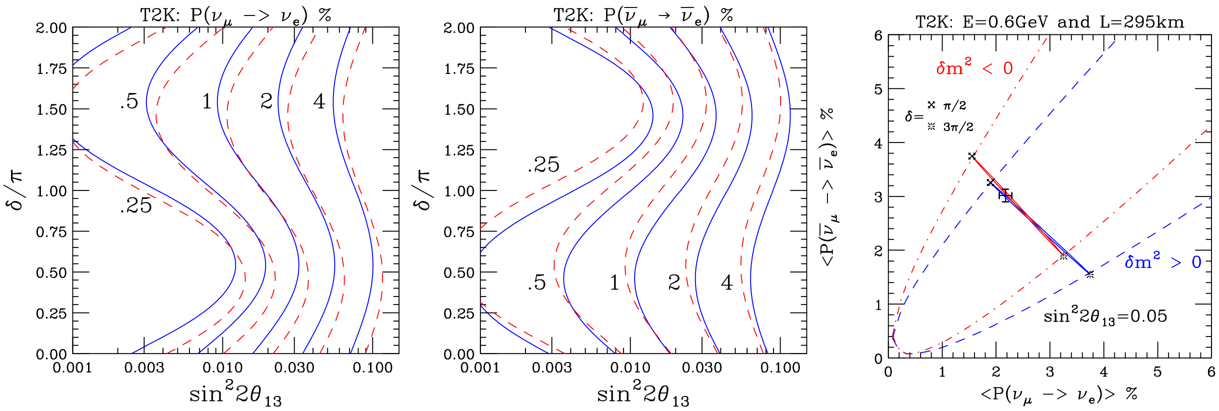

FIG. 5: The left and middle panels are the iso-probability contours for T2K as a % for the neutrino (left) and anti-neutrino (right) channels. The solid (blue) line is for the normal hierarchy whereas the dashed (red) line is for the inverted hierarchy. The right panel is the bi-probability plot showing the correlation between the two probabilities. The matter effect is small but non-negligible for T2K.

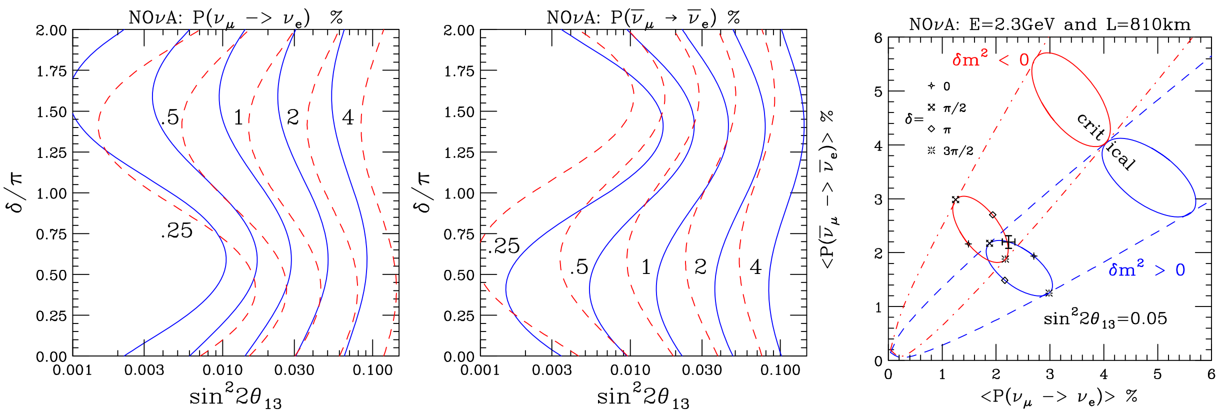

FIG. 6: The left and middle panels are the iso-probability contours for NOνA as a % for the neutrino (left) and anti-neutrino (right) channels. The solid (blue) line is for the normal hierarchy whereas the dashed (red) line is for the inverted hierarchy. The right panel is the bi-probability plot showing the correlation between the two probabilities. The matter effects and hence the separation between the hierarchies is 3 times large for T2K than NOνA primarily due to the fact NOνA has three times the baseline as T2K. The difference in the matter effect between T2K and NOνA can be used to untangle CP violation and the mass hierarchy.

and ν_μ disappearance probabilities are given by

$$\begin{aligned} P(\nu_\alpha \to \nu_\alpha) &= P(\bar\nu_\alpha \to \bar\nu_\alpha) \\ &\approx 1 - 4|U_{\alpha 5}|^2 \sin^2 \Delta_{51} - 4|U_{\alpha 4}|^2 \sin^2 \Delta_{41} + \mathcal{O}((|U_{\alpha 4}|^2 + |U_{\alpha 5}|^2)^2) \end{aligned} \tag{29}$$

where $\nu_\alpha = \nu_e$ or ν_μ. The spreading of the limit on the disappearance probabilities between two distinct δm^2, δm^2_{41} and δm^2_{51}, reduces the severity of the constraints on the appearance modes compared to the 3+1 models. An improvement on the limit of both disappearance modes by a factor of $\sqrt{2}$ would improve the constraint on the appearance mode by a factor of 2 for all values of the CP violating phase δ_{54}.

VI. SUMMARY AND CONCLUSION

A summary of neutrino oscillation phenomenology has been presented in the neutrino Standard Model - 3 active neutrinos only. The oscillation probabilities in the disappearance channels for ν_e and ν_μ flavors are presented with the relevant approximations for the experiments that will be discussed later in this volume. The appearance probability for $\nu_\mu \to \nu_e$ and $\bar{\nu}_\mu \to \bar{\nu}_e$ is discussed in some detail with particular attention to the unresolved questions associated with the neutrino mass hierarchy and CP violation. This channel is the most likely one to provide the first observation of genuine three flavor effects.

Beyond the 3 flavor Standard Model, the addition of one or more sterile neutrinos has been discussed. In these models, there are additional L/E's for which oscillation phenomena can potentially be observed and if there are more than one additional neutrino CP violating effects can be important.

[1] Z. Maki, M. Nakagawa and S. Sakata, Prog. Theor. Phys. **28**, 870 (1962).

[2] W. M. Yao *et al.* [Particle Data Group], J. Phys. G **33**, 1 (2006).

[3] See other reviews in this volume.

[4] O. Mena and S. J. Parke, Phys. Rev. D **69**, 117301 (2004) [arXiv:hep-ph/0312131].

[5] K. Eguchi *et al.* [KamLAND Collaboration], Phys. Rev. Lett. **90**, 021802 (2003). T. Araki *et al.* [KamLAND Collaboration], Phys. Rev. Lett. **94**, 081801 (2005).

[6] M. Apollonio *et al.* [CHOOZ Collaboration], Phys. Lett. B **466**, 415 (1999).

[7] F. Boehm *et al.*, Phys. Rev. D **64**, 112001 (2001) [arXiv:hep-ex/0107009].

[8] F. Ardellier *et al.* [Double Chooz Collaboration], arXiv:hep-ex/0606025.

[9] See review in this volume.

[10] H. Nunokawa, S. J. Parke and R. Zukanovich Funchal, Phys. Rev. D **72**, 013009 (2005) [arXiv:hep-ph/0503283]. H. Minakata, H. Nunokawa, S. J. Parke and R. Zukanovich Funchal, Phys. Rev. D **74**, 053008 (2006) [arXiv:hep-ph/0607284].

[11] L. Wolfenstein, Phys. Rev. D **17**, 2369 (1978) and Neutrino 1978, pg C3-C6 edited by E. C. Fowler. S. P. Mikheyev and A. Yu. Smirnov, Yad. Fiz. **42**, 1441 (1985) [Sov. J. Nucl. Phys. **42**, 913 (1985)]; Nuovo Cim. C **9**, 17 (1986).

[12] B. Aharmim *et al.* [SNO Collaboration], arXiv:nucl-ex/0502021. Also in this volume.

[13] S. J. Parke, Phys. Rev. Lett. **57**, 1275 (1986); S. J. Parke and T. P. Walker, Phys. Rev. Lett. **57**, 2322 (1986).

[14] H. Nunokawa, S. J. Parke and R. Zukanovich Funchal, Phys. Rev. D **74**, 013006 (2006) [arXiv:hep-ph/0601198].

[15] K. S. Hirata *et al.* [KAMIOKANDE-II Collaboration], Phys. Rev. Lett. **65**, 1297 (1990); M. B. Smy *et al.* [Super-Kamiokande Collaboration], Phys. Rev. D **69**, 011104 (2004); J. Hosaka *et al.* [Super-Kamkiokande Collaboration], arXiv:hep-ex/0508053.

[16] E. Aliu *et al.* [K2K Collaboration], Phys. Rev. Lett. **94**, 081802 (2005) [arXiv:hep-ex/0411038].

[17] D. G. Michael *et al.* [MINOS Collaboration], Phys. Rev. Lett. **97**, 191801 (2006) [arXiv:hep-ex/0607088].

[18] Y. Itow *et al.*, arXiv:hep-ex/0106019.

[19] D. S. Ayres *et al.* [NOvA Collaboration], arXiv:hep-ex/0503053.

[20] A. Cervera, A. Donini, M. B. Gavela, J. J. Gomez Cadenas, P. Hernandez, O. Mena and

S. Rigolin, Nucl. Phys. B **579**, 17 (2000) [Erratum-ibid. B **593**, 731 (2001)] [arXiv:hep-ph/0002108].
[21] A. Aguilar *et al.* [LSND Collaboration], Phys. Rev. D **64**, 112007 (2001) [arXiv:hep-ex/0104049].
[22] A. A. Aguilar-Arevalo *et al.* [The MiniBooNE Collaboration], arXiv:0704.1500 [hep-ex].
[23] G. Karagiorgi, A. Aguilar-Arevalo, J. M. Conrad, M. H. Shaevitz, K. Whisnant, M. Sorel and V. Barger, Phys. Rev. D **75**, 013011 (2007) [arXiv:hep-ph/0609177].